

17 Aug 2005

PM Emission From a Commercial Jet Engine -- Project APEX

Donald E. Hagen

Missouri University of Science and Technology, hagen@mst.edu

Philip D. Whitefield

Missouri University of Science and Technology, pwhite@mst.edu

Prem Lobo

Missouri University of Science and Technology, plobo@mst.edu

Max B. Trueblood

Missouri University of Science and Technology, trueblud@mst.edu

Follow this and additional works at: https://scholarsmine.mst.edu/phys_facwork

 Part of the [Chemistry Commons](#), and the [Physics Commons](#)

Recommended Citation

D. E. Hagen et al., "PM Emission From a Commercial Jet Engine -- Project APEX," *Proceedings of the 9th ETH Conference on Combustion Generated Nanoparticles (2005, Zurich, Switzerland)*, Aug 2005.

This Article - Conference proceedings is brought to you for free and open access by Scholars' Mine. It has been accepted for inclusion in Physics Faculty Research & Creative Works by an authorized administrator of Scholars' Mine. This work is protected by U. S. Copyright Law. Unauthorized use including reproduction for redistribution requires the permission of the copyright holder. For more information, please contact scholarsmine@mst.edu.

PM EMISSIONS FROM A COMMERCIAL JET ENGINE – PROJECT APEX

Donald Hagen, Philip Whitefield, Prem Lobo, and Max Trueblood
University of Missouri - Rolla

Project APEX (Aircraft Particle Emissions eXperiment) was a multi-agency commercial aircraft emission characterization and technology demonstration experiment. Its objective was to characterize particle and trace gas precursor species in the emissions from a NASA DC-8 aircraft with General Electric CFM56-2C1 engines at the engine exit plane as well as selected down stream locations. This was to advance the understanding of particle emissions and their evolution in the atmosphere from a current in-service turbofan engine. The test was conducted at the NASA Dryden Flight Research Center at Edwards Air Force Base California during April 15-30, 2004. Participants included the National Aeronautics and Space Administration, Environmental Protection Agency, Federal Aviation Administration, Department of Defense, the aviation industry (General Electric, Pratt and Whitney, and Boeing), and the research community (Aerodyne Research Inc., Massachusetts Institute of Technology, Process Metrix, University of California-Riverside, and University of Missouri-Rolla).

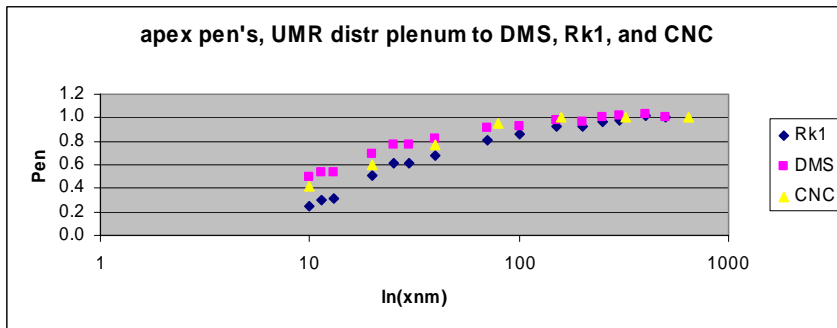
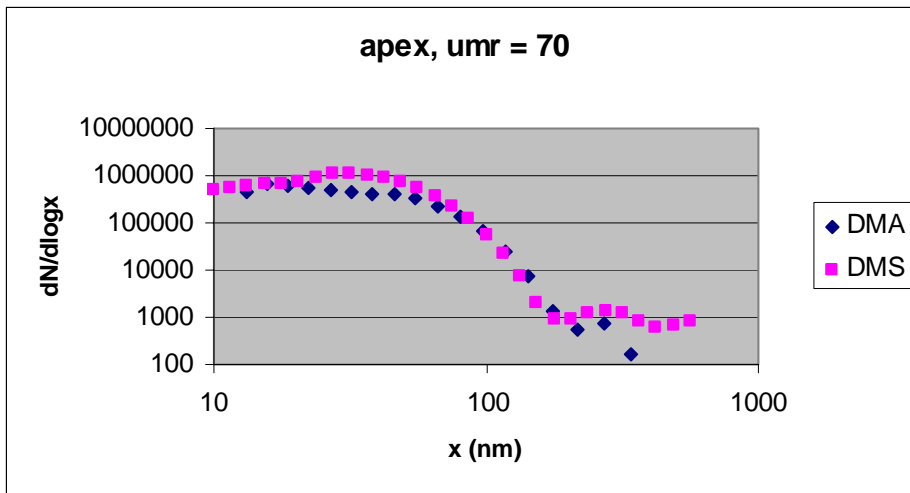
The test was conducted on the ground with sampling rakes behind the engine at selected locations. The engine was operated at various power settings ranging from 4% to 100% thrust, with three classes of fuels: baseline JP8 (409 ppm sulfur and 17.5% aromatic), high sulfur (1639 ppm sulfur and 17.5% aromatic), and high aromatic (Jet A with 553 ppm sulfur and 22% aromatic). The engine was held at each test condition for 4 minutes, except for the 100% condition which was limited to 1.5 minutes. Each condition was visited multiple times during the campaign.

A new instrument, the DMS500, for fast real-time analysis of the size distribution, shape parameters, number density, mass concentration and number- and mass-based emission indices of exhaust particulates was employed, and here we report a comparison of its results with traditional instrumentation, the scanning differential mobility spectrometer (TSI Model 3071) and the condensation nuclei counter (TSI Model 3022). The samples were collected with probes mounted behind the engine exhaust plane (the intercomparison focused on data from a probe 1m behind the engine), and were delivered via a sampling train to a distribution plenum in the UMR instrument trailer. From there they were delivered to the various instruments. For the intercomparison, each instrument's measurements were corrected for losses back to the distribution manifold, using size dependent line penetration calibration data. Differences between instruments varied substantially from run to run (see plot of PctDXb vs. umr). Most of these large differences were associated with runs having low signal to noise ratios or signal instability. A weight function was devised to account for these issues, and weighted average percent differences and rms percent differences were evaluated for three aerosol parameters: number and mass based geometric mean diameters, and total number concentration. The DMS500 agreed well with traditional slower instrumentation. For number based geometric mean diameter, the DMS tended to be slightly below the DMA, by 3% on average, with a 12% scatter (rms average difference). For mass weighted geometric mean diameter, the DMS was systematically low, by 8% on average, with a 15% rms difference. For total particle concentration, the DMS was systematically high

by 60% in comparison to the TSI model 3022, with a rms difference of 61%. This is comparable to the difference seen by Kittleson et.al. (D. Kittleson, T. Hands, C. Nickolaus, N. Collings, V. Niemela, and M. Twigg, "Mass correlation of engine emissions with spectral instruments", JSAE Paper No. 20045462) between a DMS500 and a TSI CPC for diesel emissions.

Aerosol parameters did show dependencies on power, fuel type, and distance behind engine exit plane. The geometric mean diameter was observed to increase monotonically with power for all fuels, and ranged from 15 to 34 nm. The geometric standard deviation (σ) generally increased with power for all fuels, ranging from 1.5 to 1.8. This represents a factor 3 to 4 increase in halfwidth. The number based emission index (EIn) had a maximum at low power and was larger at 30m than at 1m for low and mid-range power. EIn for 1m and 30m converged at high power, where the temperatures are highest and plume residence times are lowest. This is compatible with gas-to-particle conversion being active in the plume. The mass based emission indices also exhibited this trend, converging at high power and diverging at low power, although not as strongly as for the number based emission indices.

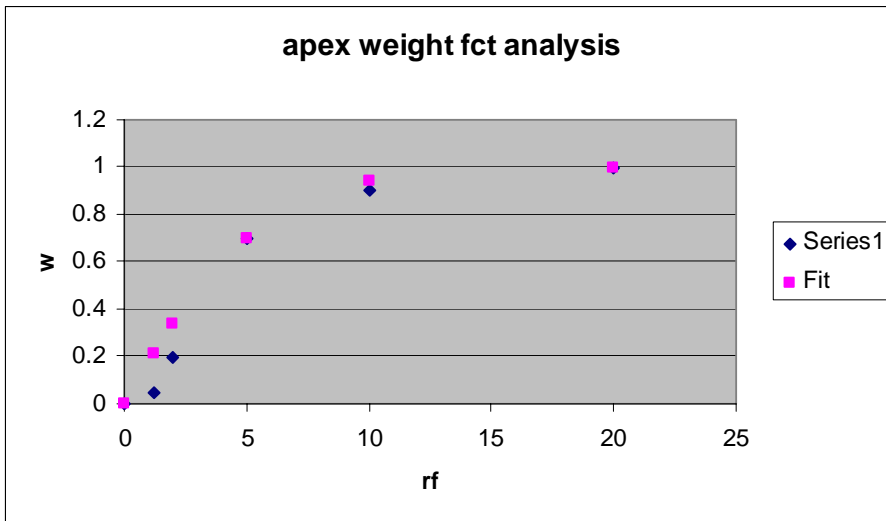
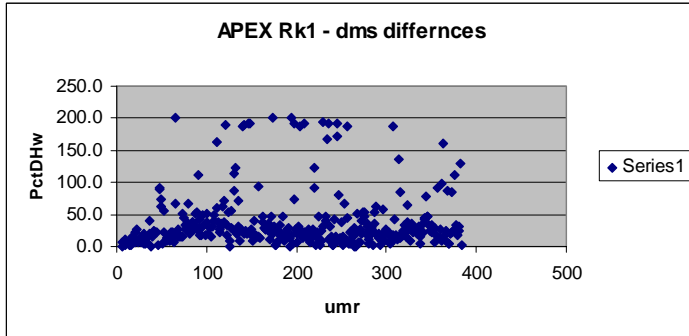
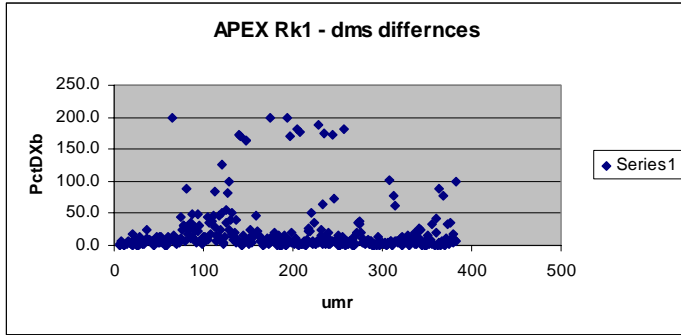
The hydration properties of the exhaust aerosol were characterized using deliquescence measurements with a tandem DMA system. The original dry (40 nm and 60 nm) and deliquesced size information was converted into soluble mass fraction assuming sulfuric acid as the soluble species. The average (over size and power) soluble mass fractions are plotted vs. probe distance behind the engine (smf vs. PLoc). No statistically significant soluble material was observed at the 1m and 10m locations, for any fuel type. For the 30m probe, soluble material was found, with soluble mass fractions of 0.057 ± 0.026 for the baseline fuel, 0.115 ± 0.076 for the aromatic fuel, and 0.151 ± 0.085 for the Hi sulfur fuel. This hydration behavior is compatible with gas-to-particle conversion being active in the plume.

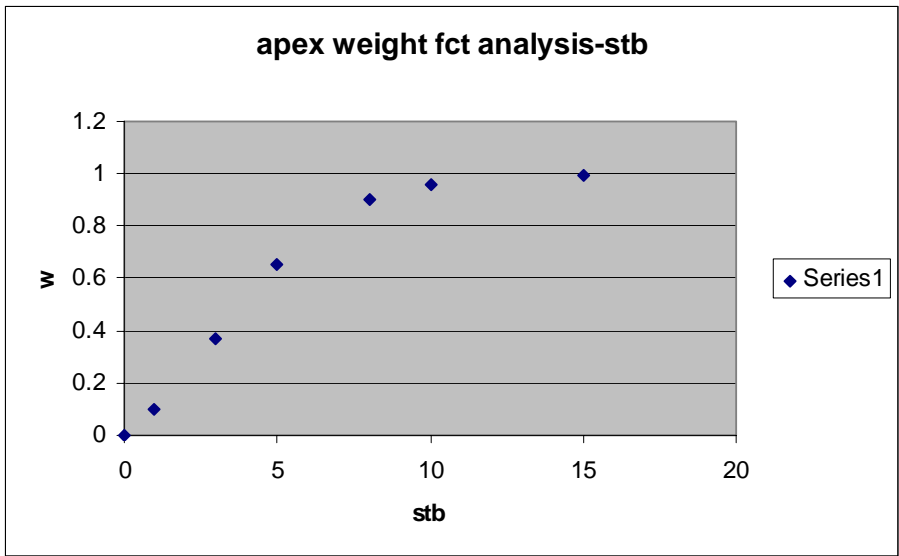


$$\text{pen2(Rk1)} = \frac{-0.04954 \cdot (\ln x)^2 + 0.6118 \cdot (\ln x) - 0.8963}{1} \quad \begin{array}{l} \text{if } x_{nm} < 500 \\ \text{if } x_{nm} > 500 \end{array}$$

$$\text{pen2(dms)} = \frac{-0.04036 \cdot (\ln x)^2 + 0.4735 \cdot (\ln x) - 0.3787}{1} \quad \begin{array}{l} \text{if } x_{nm} < 210 \\ \text{if } x_{nm} > 210 \end{array}$$

$$\text{pen3(cnc)} = \frac{0.2539 \cdot (\ln x) - 0.1647}{1} \quad \begin{array}{l} \text{if } x_{nm} < 98 \\ \text{if } x_{nm} > 98 \end{array}$$

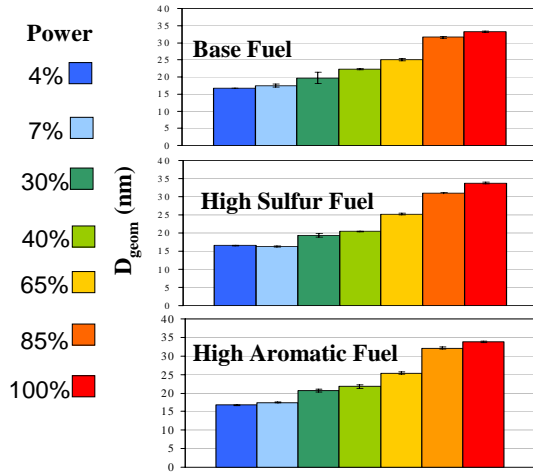




DMS-DMA Intercomparison

Parameter	Avg Pct Diff	RMS Pct Diff
Dgn	-3	12
Dgm	-8	15
TCN	60	61

D_{geom} vs. Power Ploc 1m, NASA Sequences

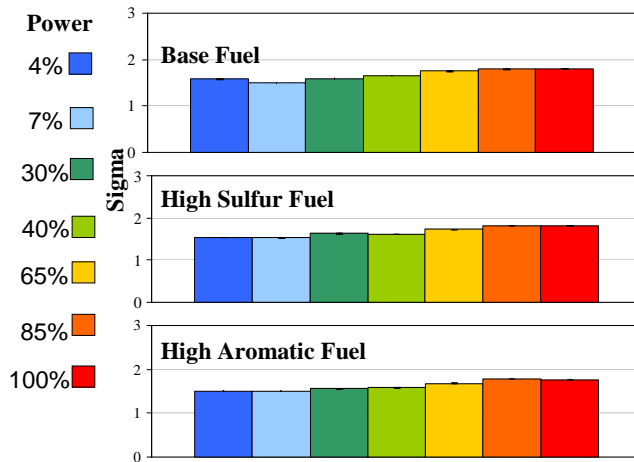


D_{geom}

- D_{geom} increases monotonically with power for all 3 fuels and ranges from 15 ~ 34nm
- The increase for the high sulfur and high aromatic fuels is greater than that for the Base fuel by ~6-7%

Sigma (geometric standard deviation) vs. Power Ploc 1m, NASA Sequences

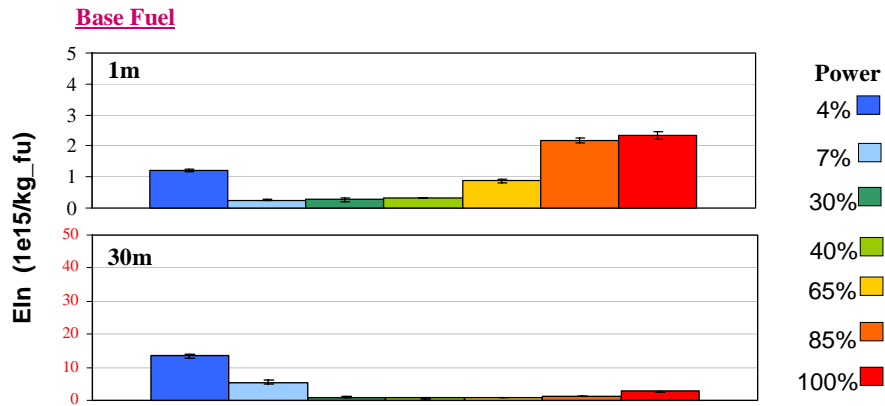
Half width = D_{geom} (Sigma -1)



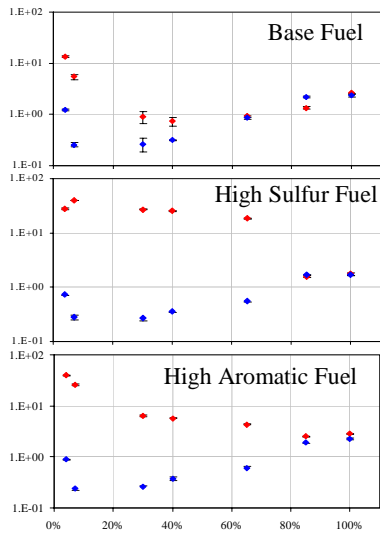
Sigma

- Sigma generally increases with power for all 3 fuels and ranges from 1.5 ~ 1.8
- This increase in Sigma represents a factor of 3-4 increase in half width from 7.5 - 26.4nm

EIn (1e15/kg_fu) vs. Power Ploc 1m and 30m, NASA Sequences



EIn (1e15/kg_fu) vs. Power NASA Sequences



Probe
1m ◆
30m ◆

Max EIn at low power

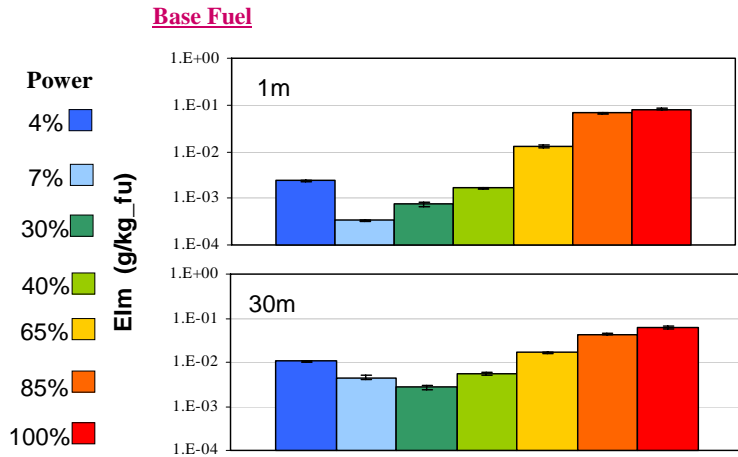
EIn higher at 30m than 1m

1m and 30m EIn converge at high power.

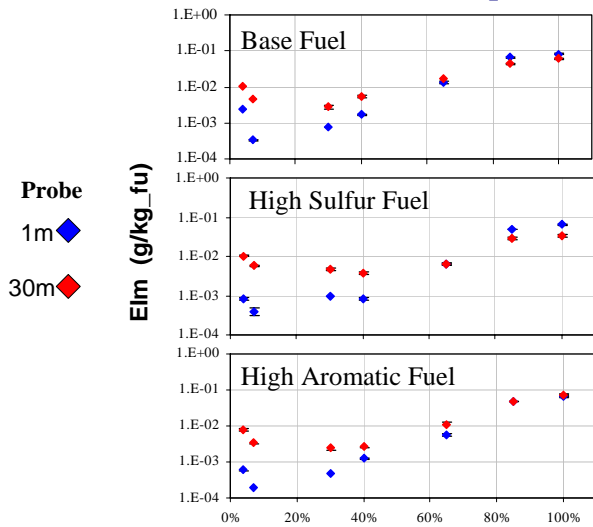
Largest separation at low power.

Suggests gas-to-particle conversion.

EIm (g/kg_fu) vs. Power, Ploc 1m and 30m, NASA Sequences



EIm (g/kg_fu) vs. Power NASA Sequences



At high power, the EIm's for the 1 and 30m cases converge suggesting that the mass at high power is dominated by the non-volatile aerosol component

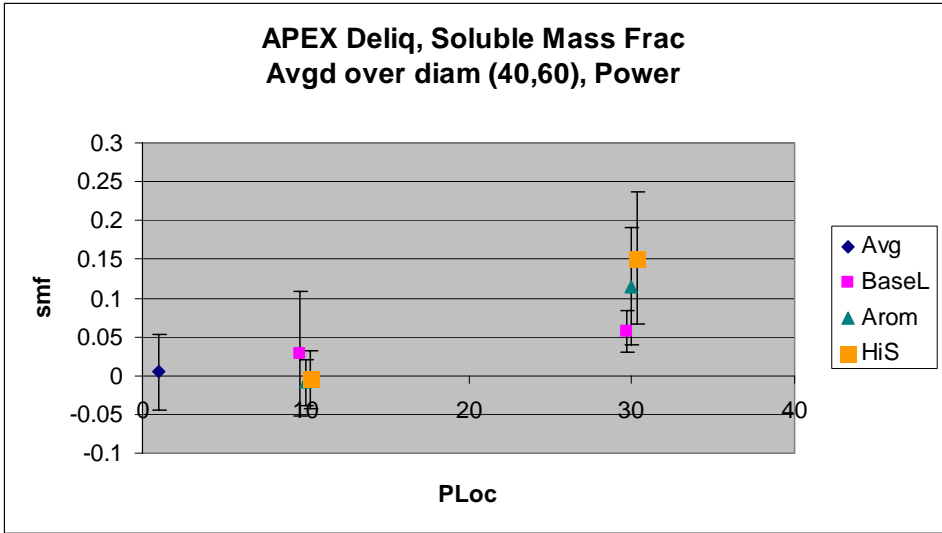


Fig 2. Soluble mass fraction v. probe position from UMR Deliq.

PM Emission From a Commercial Jet Engine – Project APEX

- Donald Hagen, Philip Whitefield, Prem Lobo, and Max Trueblood
- Cloud and Aerosol Sciences Laboratory
- Depts of Physics and Chemistry
- University of Missouri – Rolla

Aircraft Particle Emissions eXperiment (APEX)

A Multi-Agency
Commercial Aircraft Emission Characterization
and
Technology Demonstration Experiment



Objectives

To characterize particle and trace gas precursor species from the NASA aircraft DC-8 with CFM56-2C1 engines at the engine exit plane as well as at selected down stream locations to advance the understanding of particle emissions and their evolution in the atmosphere from a current in-service turbofan engine

Test Location

NASA DFRC @ Edwards AFB, CA

Test Period

April 15 – 30, 2004

Test Aircraft/Engine

NASA DC-8 with CFM56-2C1 engine

Team

Participants:

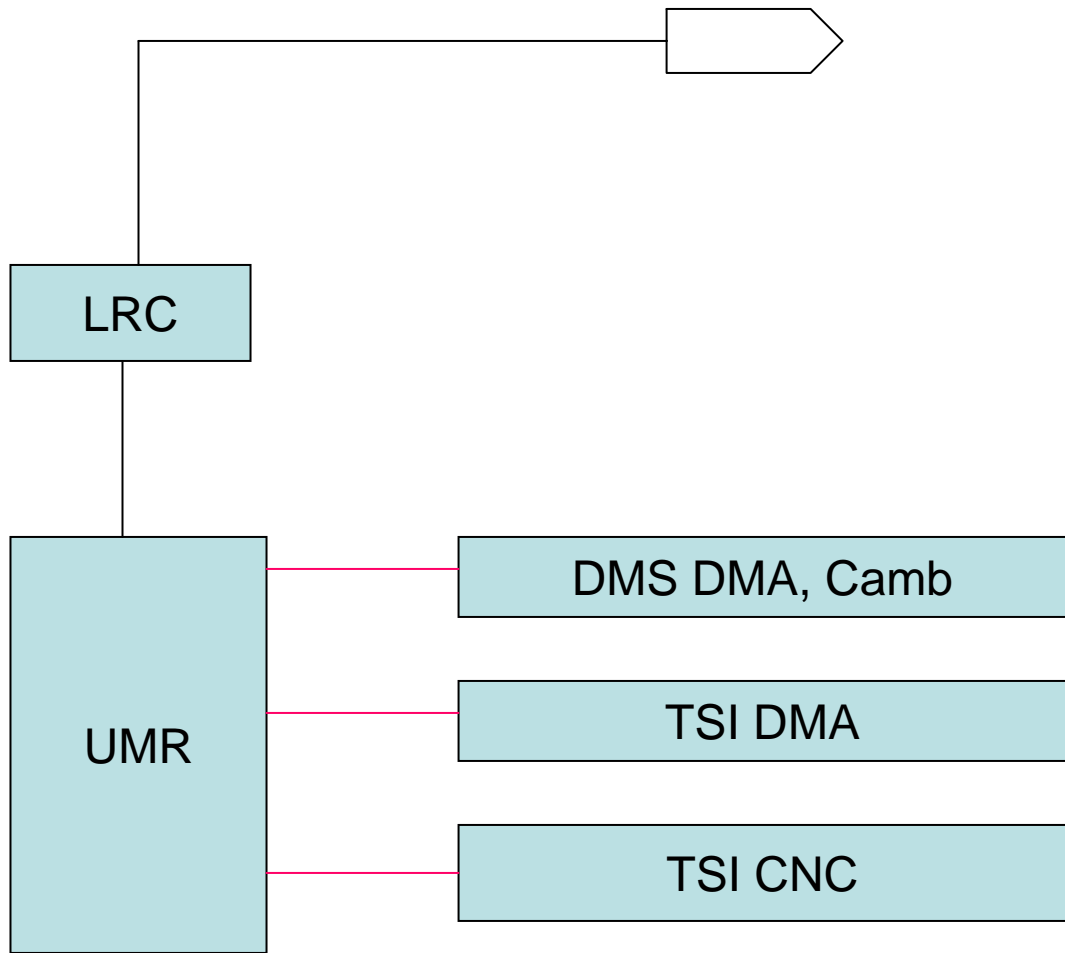
**NASA (DFRC, GRC, LaRC), EPA, FAA,
DoD (AEDC, NAVAIR, NFESC, WPAFB),
Aviation Industry (GE, Boeing, PW),
Research community (ARI, MIT, PM, UCR, UMR)**

**Sponsors: NASA
EPA
DOD**

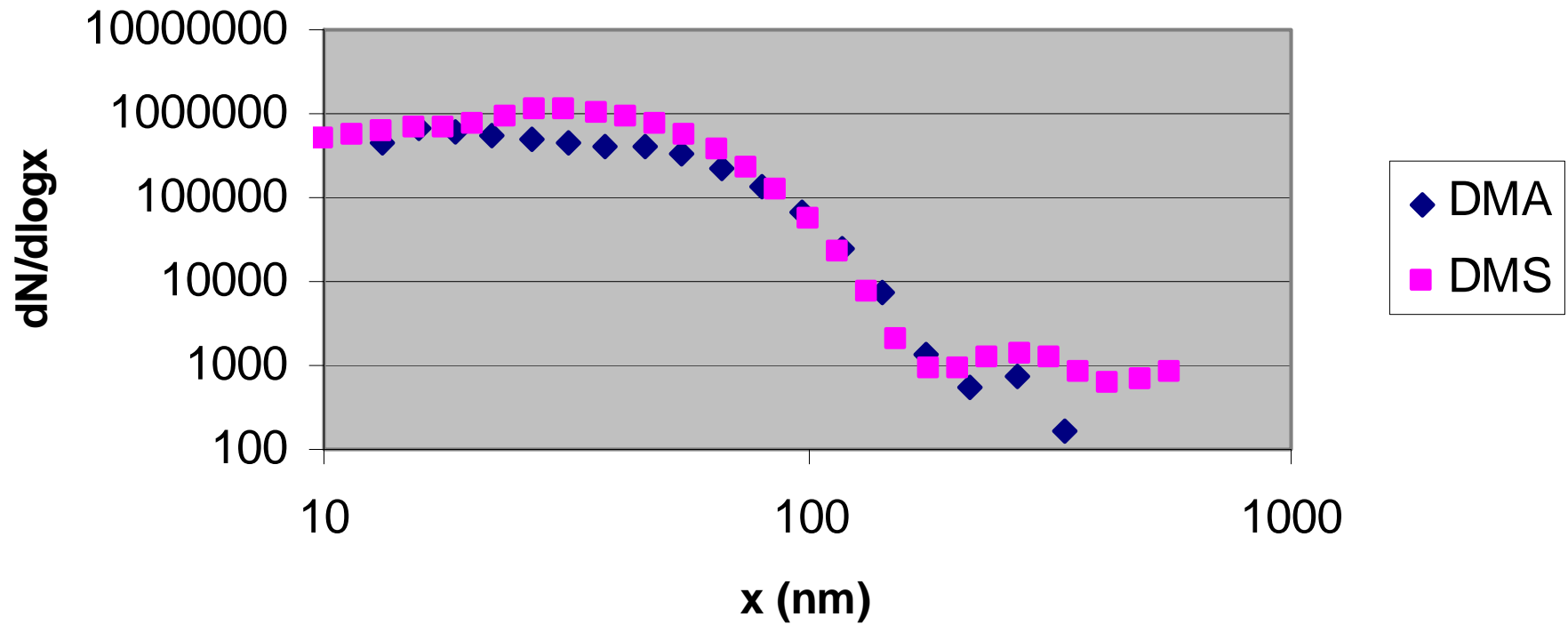
**Manager: Dr. Chowen Chou Wey
NASA GRC**



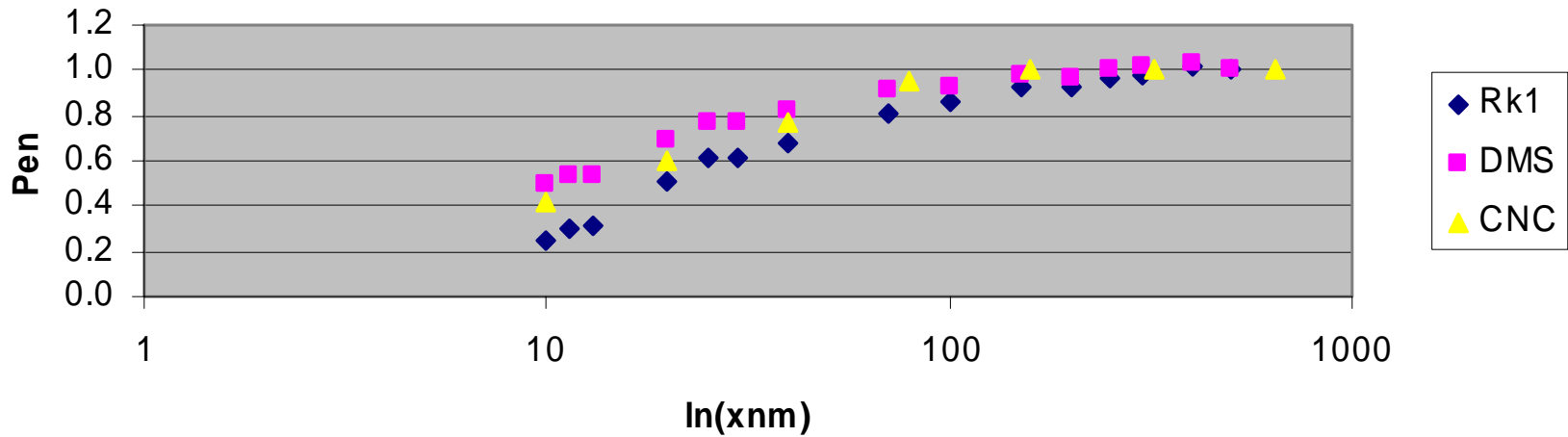




apex, umr = 70



apex pen's, UMR distr plenum to DMS, Rk1, and CNC



$$\text{pen2(Rk1)} = \frac{-0.04954 \cdot (\ln x)^2 + 0.6118 \cdot (\ln x) - 0.8963}{1} \quad \begin{array}{l} \text{if } x_{nm} < 500 \\ \text{if } x_{nm} > 500 \end{array}$$

$$\text{pen2(dms)} = \frac{-0.04036 \cdot (\ln x)^2 + 0.4735 \cdot (\ln x) - 0.3787}{1} \quad \begin{array}{l} \text{if } x_{nm} < 210 \\ \text{if } x_{nm} > 210 \end{array}$$

$$\text{pen3(cnc)} = \frac{0.2539 \cdot (\ln x) - 0.1647}{1} \quad \begin{array}{l} \text{if } x_{nm} < 98 \\ \text{if } x_{nm} > 98 \end{array}$$

Percent differences between instruments

APEX 383 runs ($u=1,2,3,\dots,383$)

$\{x_j, sn_j\}_{dms,u} \implies Dgn_{dms,u} \quad Dgm_{dms,u} \quad TCN_{dms,u}$

$\{x_j, sn_j\}_{tsi,u} \implies Dgn_{tsi,u} \quad Dgm_{tsi,u}$

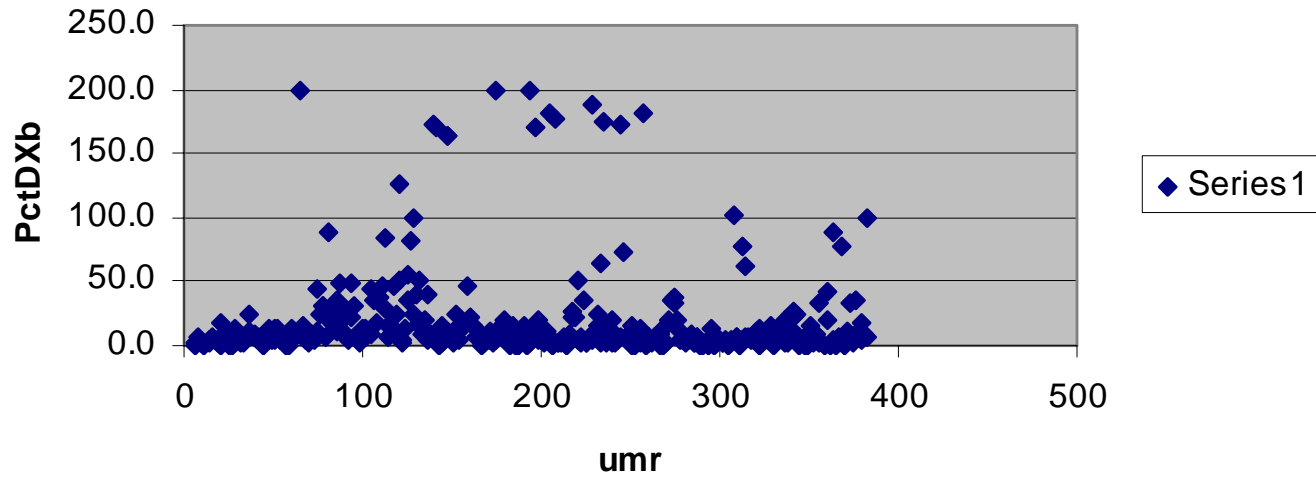
TCN_{cnc}

$PctDgn_u \implies 200 \cdot (Dgn_{dms,u} - Dgn_{tsi,u}) / (Dgn_{dms,u} + Dgn_{tsi,u})$

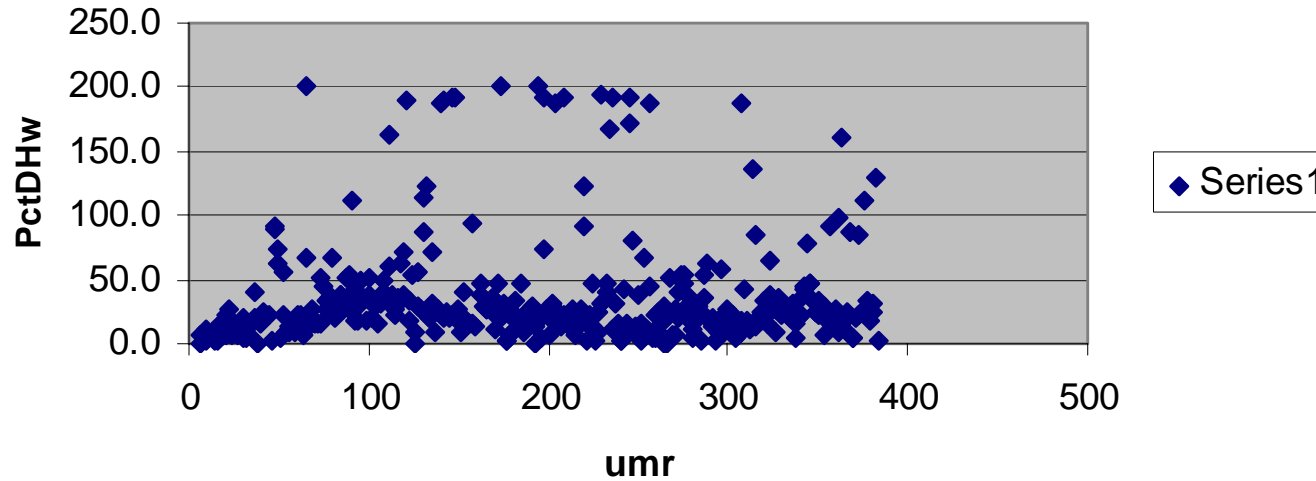
$PctDgm_u \implies 200 \cdot (Dgm_{dms,u} - Dgm_{tsi,u}) / (Dgm_{dms,u} + Dgm_{tsi,u})$

$PctTCN_u \implies 200 \cdot (TCN_{dms,u} - TCN_{cnc}) / (TCN_{dms,u} + TCN_{cnc})$

APEX Rk1 - dms differnces



APEX Rk1 - dms differnces



Uncertainty metrics

Quantify the uncertainty in the measurements for a given run (u).

Stb = Signal to background.

PctDDg Differences between 2 TSI DMA size sweeps.

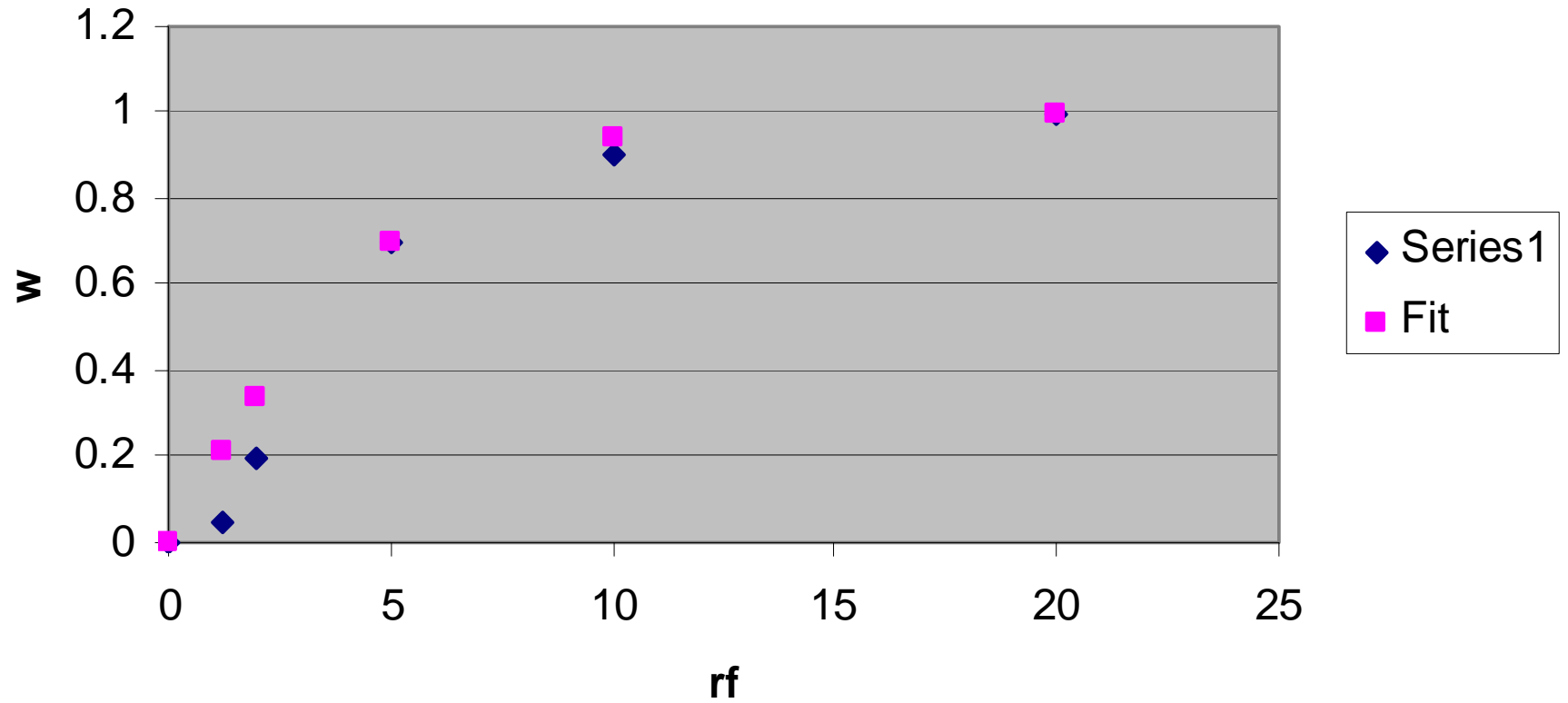
$Dg_{dms}, \sigma_{Dg,dms}$ From average of ~ 20 sweeps.

Build a weight function that will give a large weight to good data having low uncertainty and small credit to marginal data having high uncertainty.

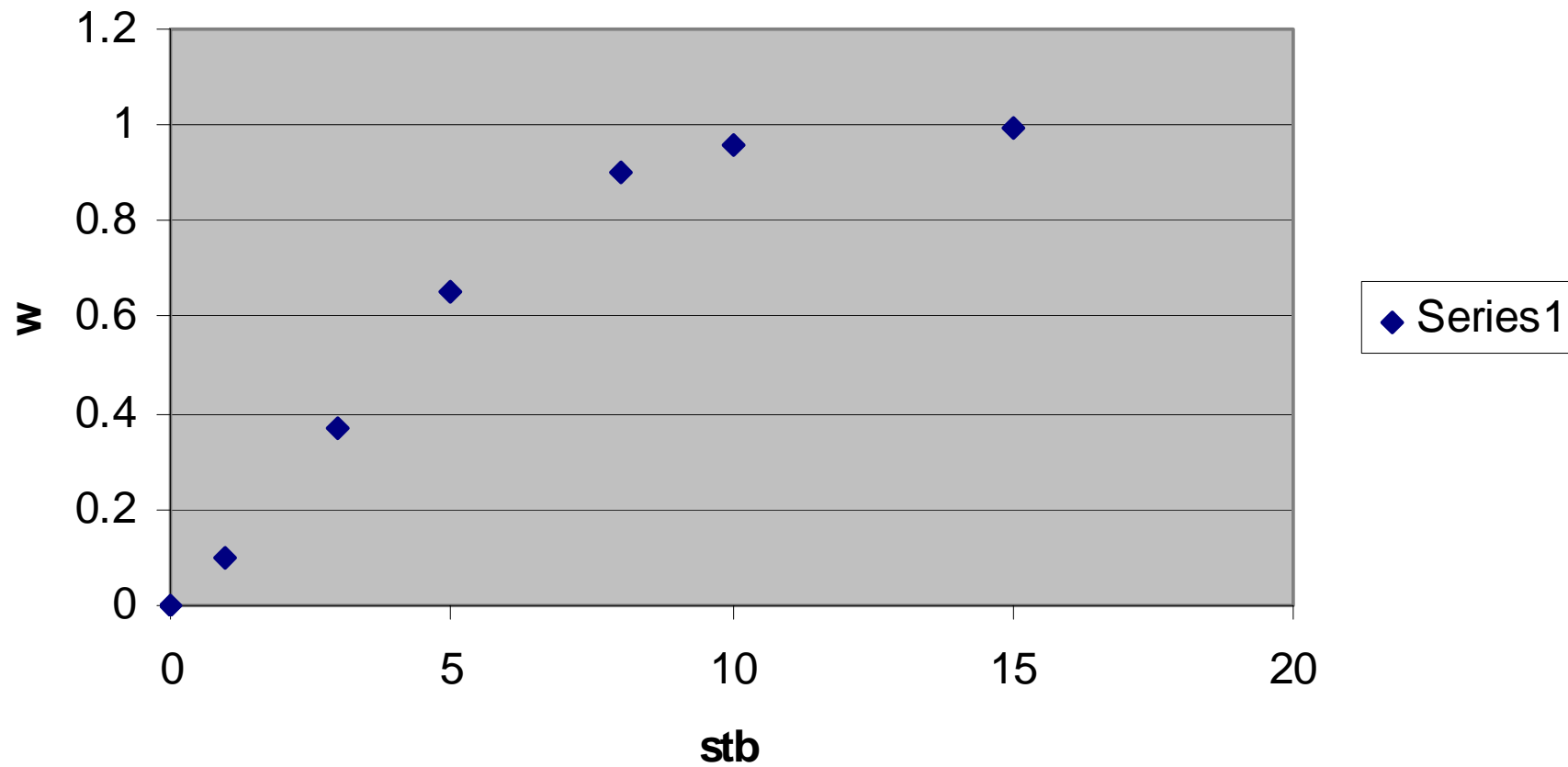
Convert these uncertainty parameters into ones that increase with goodness of the data:

Stb, $100/PctDg$, $Dg_{dms}/\sigma_{Dg,dms}$
rf reciprocal fractional errors

apex weight fct analysis



apex weight fct analysis-stb



Global weight function:

$$w_Dgn = w_ (100/PctDg) * w_ (Dg/sig_Dg) * w_stb$$

$$\langle PctDgn \rangle = [\Sigma PctDgn * w_Dgn] / [[\Sigma w_Dgn]$$

$$rms PctDgn = Sqrt \{ [\Sigma PctDgn^2 * w_Dgn] / [[\Sigma w_Dgn] \}$$

DMS-DMA Intercomparison

Parameter	Avg Pct Diff	RMS Pct Diff
Dgn	-3	12
Dgm	-8	15
TCN	60	61

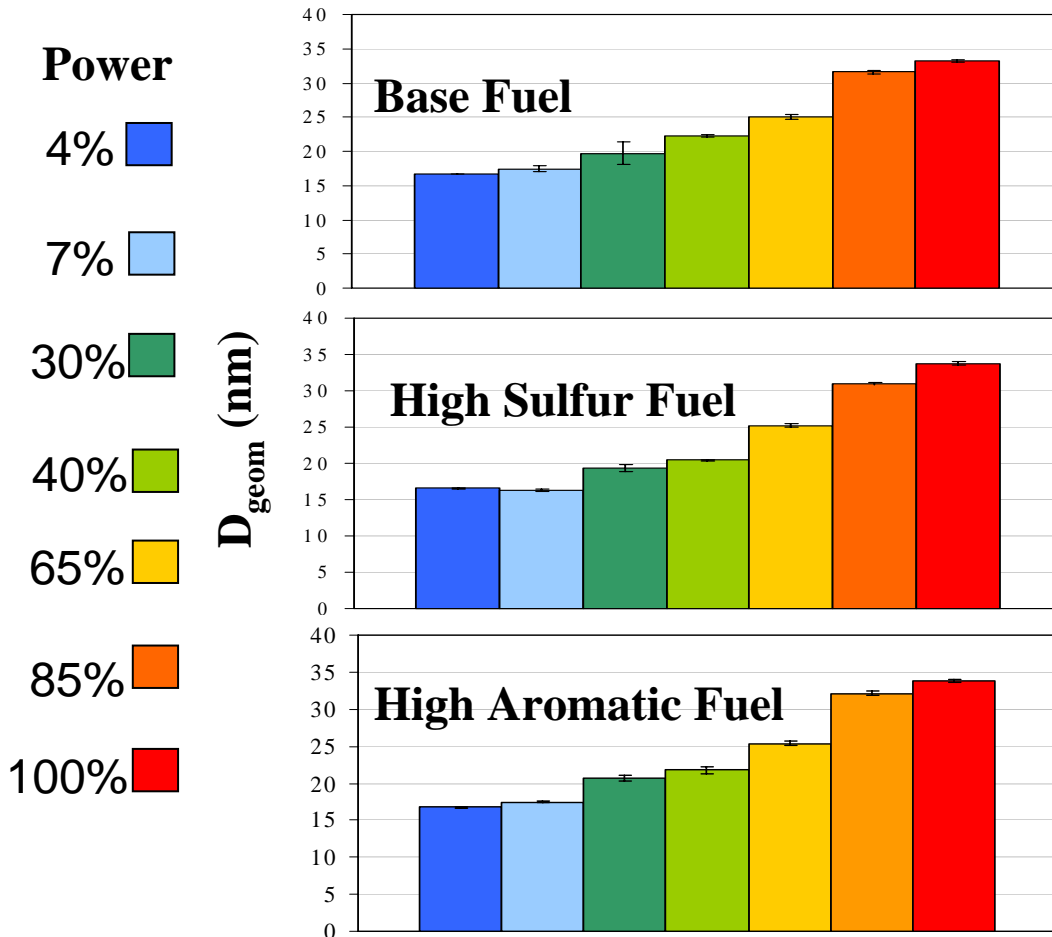
Intercomparison Summary

- The DMS500 agreed well with traditional slower instrumentation.
- For geometric mean diameter, the DMS tended to be slightly below the DMA, by 3% on average, with a 12% scatter (rms average difference).
- For mass weighted geometric mean diameter, the DMS was systematically low (by 8% on average), and the rms difference was 15%.

- For total particle concentration, the DMS was systematically high by 60% in comparison to the TSI model 3022, with a rms difference of 61%.
- Comparable difference (59%) to that seen by Kittleson et.al. between DMS500 and a TSI CPC for diesel emissions.

D_{geom} vs. Power

Ploc 1m, NASA Sequences



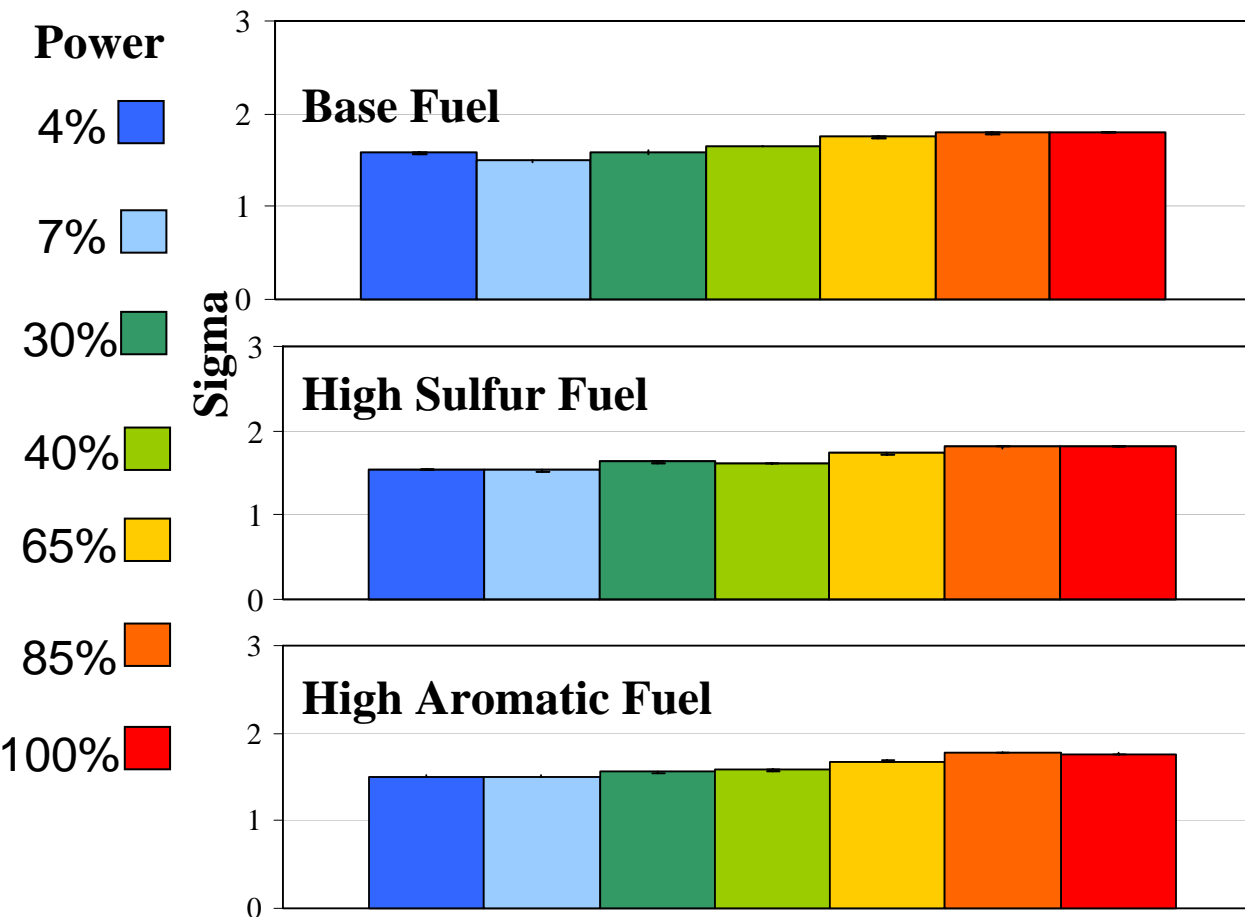
D_{geom}

- D_{geom} increases monotonically with power for all 3 fuels and ranges from 15 ~ 34nm
- The increase for the high sulfur and high aromatic fuels is greater than that for the Base fuel by ~6-7%

Sigma (geometric standard deviation) vs. Power

Ploc 1m, NASA Sequences

Half width = $D_{geom} (\text{Sigma} - 1)$

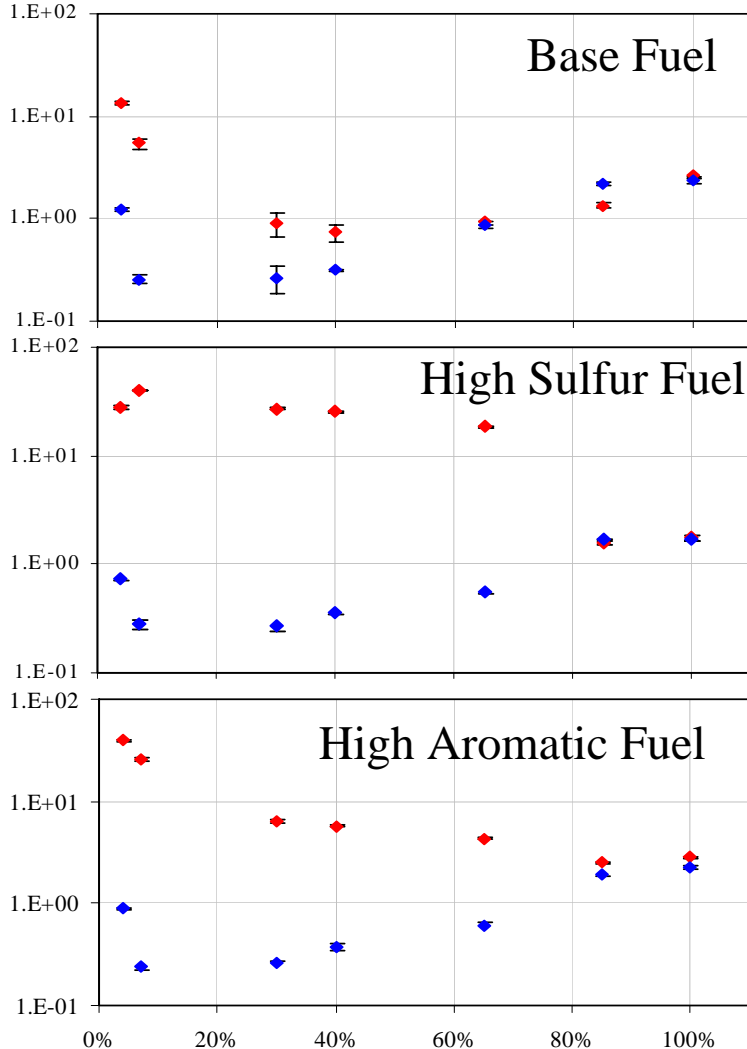


Sigma

- Sigma generally increases with power for all 3 fuels and ranges from 1.5 ~ 1.8

- This increase in Sigma represents a factor of 3-4 increase in half width from 7.5 - 26.4nm

EIn (1e15/kg_fu) vs. Power NASA Sequences



Max EIn at low power

EIn higher at 30m than 1m

1m and 30m EIn converge
at high power.

Largest separation at low
power.

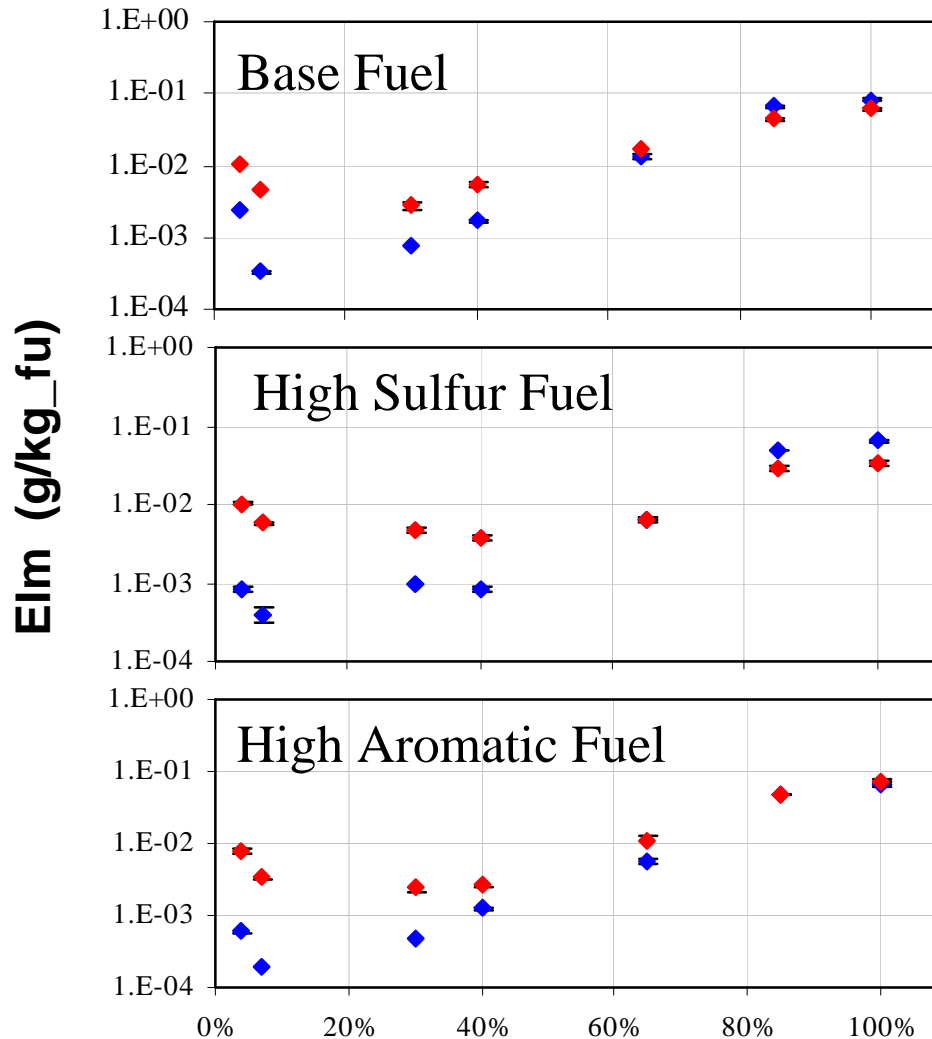
Probe

1m 

30m 

Suggests gas-to-particle
conversion.

Elm (g/kg_fu) vs. Power NASA Sequences



At high power, the Elms for the 1 and 30m cases converge suggesting that the mass at high power is dominated by the non-volatile aerosol component

Hydration Properties

- Objective – To determine the PM soluble mass fraction.
- Method - Deliquescence

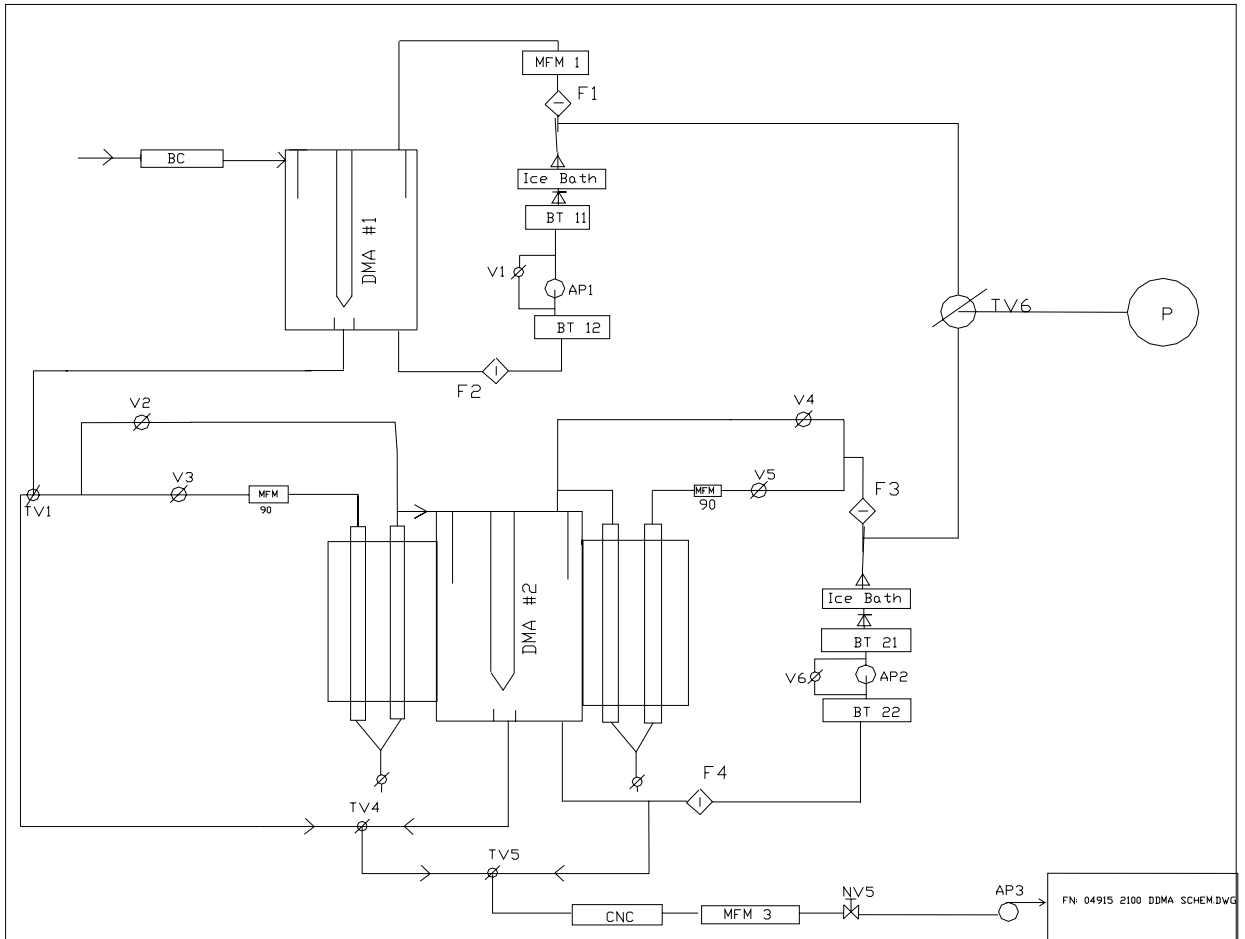


Fig. 1 Schematic of UMR deliquescence apparatus.

APEX Deliq, Soluble Mass Frac Avgd over diam (40,60), Power

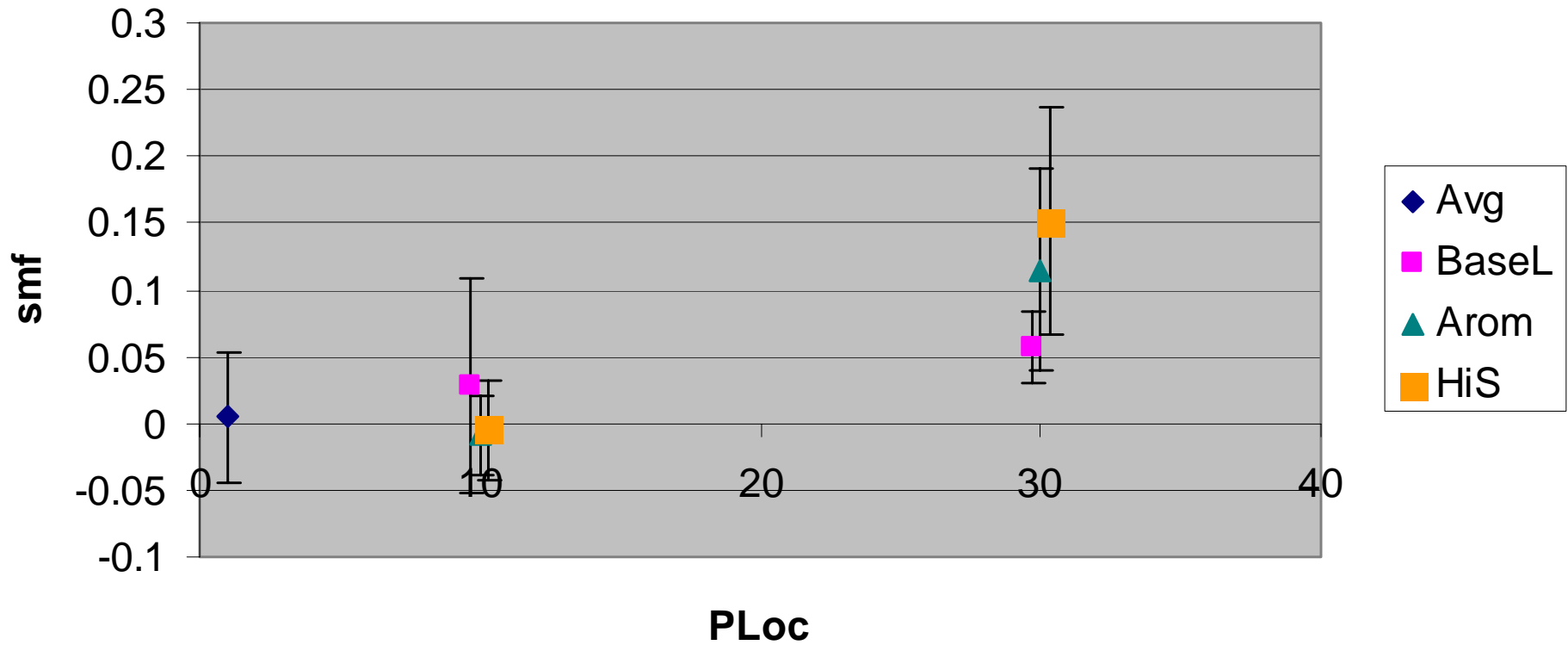


Fig 2. Soluble mass fraction v. probe position from UMR Deliq.

CONCLUSIONS:

- 1. Two classes of particles were measured. These had dry diameters of approximately 40 nm and 60 nm. The results of both classes of particle diameters and the results of all thrust settings are combined in the previous plot and the following conclusions.**
- 2. At the 10 m probe, the soluble mass fraction (sol mf) was not statistically different from that at the 1 m probe.**
- 3. At the 30 m probe, the soluble mass fraction (sol mf) was**
0.057 +/- 0.026 for the baseline fuel (overlaps with 10m),
0.115 +/- 0.076 for the aromatic fuel, and
0.151 +/- 0.085 for the Hi sulfur fuel.

Spares



Weight function for fractional error uncertainties

f = fractional error

w_f = weight function

rf = reciprocal fractional error

f	rf	w_f
inf	0	0
0.8	1.25	0.05
0.5	2	0.2
0.2	5	0.7
0.1	10	0.9
0.05	20	1

A good fit to this is given by:

$$w_f = \tanh(rf / \text{const}), \text{ const}=5.765$$

Weight function for signal to background

$$w_stb = [\tanh(stb/c1 - c2) + \tanh(c2)] / (1 + \tanh(c2))$$

(Wanted a less-sharp curve at small stb)

This is a two parameter fit, we need two data points:

stb:	1	8
w_stb	0.1	0.9

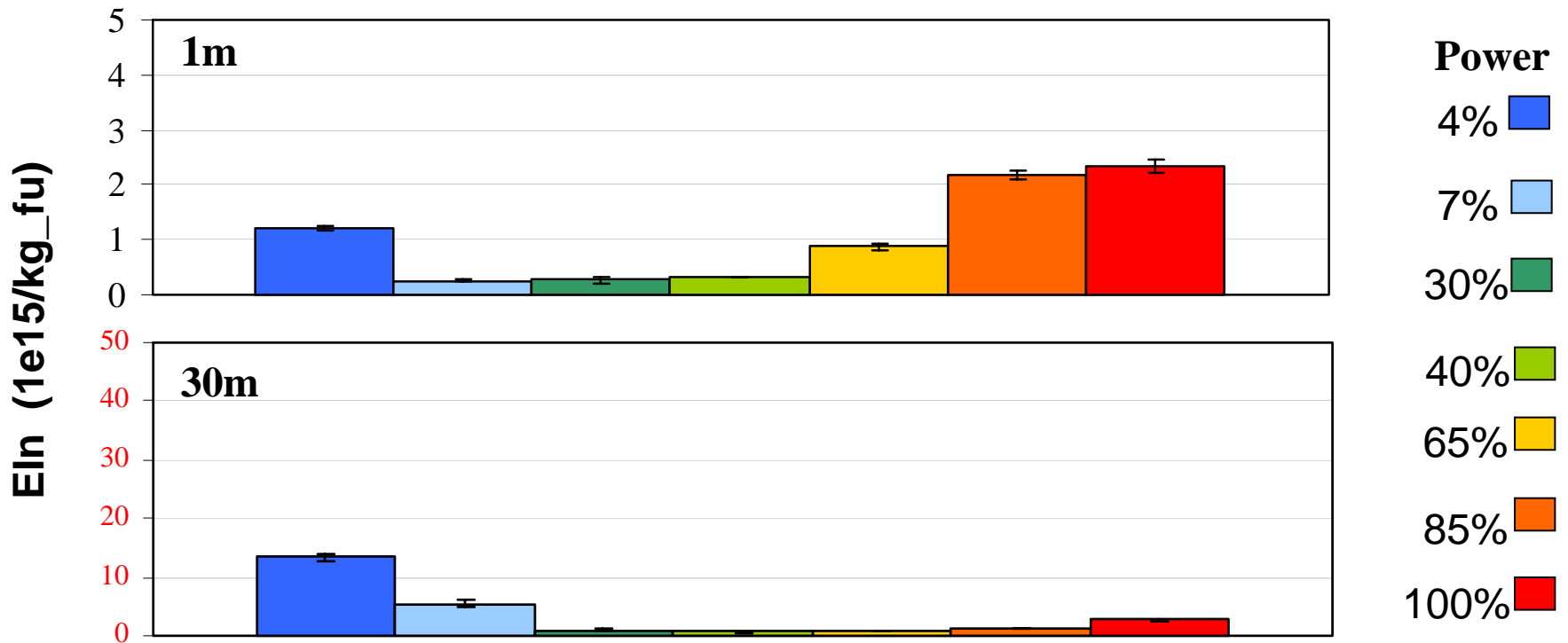
A non-linear fit yields

$$C1 = 4.02775$$

$$C2 = 0.783$$

EIn (1e15/kg_fu) vs. Power Ploc 1m and 30m, NASA Sequences

Base Fuel



EIm (g/kg_fu) vs. Power, Ploc 1m and 30m, NASA Sequences

Base Fuel

